Frontal motion in the atmosphere

By E. TURKEL, *Department of Mathematical Sciences, Tel-Aviv University, Tel-Aviv, Israel*

(Manuscript received July 12, 1973; revised version April 24, 1974)

ABSTRACT

The motion of frontal disturbances in the atmosphere is studied with a one layer non-linear model proposed by Stoker. The equations of motion are integrated in the interior of the domain by a two step method. Flows resulting from various initial and boundary are considered for considerably longer times than those previously computed. The boundary is followed by a numerical procedure that allows for arbitrary shapes of the front. Hence, flows can be followed until occlusion occurs and so we can accurately compare the effects of the various initial and boundary conditions on the occlusion process. In all cases, the cold front propagates faster than the warm front and a relatively strong mass convergence region exists behind the cold front. A cyclonic circulation pattern is clearly visible near the cold front. These facts suggest the occurrence of severe storms associated with cold fronts but not with warm fronts.

1. Introduction

In meteorology it is known that the weather in the middle latitudes is conditioned to a considerable degree by events associated with the propagation of wave-like disturbances on a discontinuity surface between warm and cold air masses in the atmosphere. The intersection of the discontinuity surface with the earth is known as a front. In this paper we will be interested in following the motion of these fronts.

The importance of nonlinear effects in the dynamical equations of the cold front were pointed out by Abdullah (1949), Freeman (1952), and Tepper (1952) who applied the method of characteristics to solve nonlinear equations in one space dimension. Later Stoker (1957) developed a two-space dimensional model, in both a single layer and a two layer version, for the motion of a frontal surface. Stoker together with Kasahara & Isaacson (1965) made some numerical calculations with the one layer model and found the beginnings of the occlusion effect. Ritter (1970) duplicated these results using a Lagrangian technique. Grammeltvedt (1970) studied the two layer model and reached similar conclusions. Kasahara & Rao (1972) have shown, on the basis of linear theory, that the full two layer model can be unstable. Grammeltvedt used a large amount of artificial dissipation in his numerical scheme which may have prevented the instabilities from arising. Therefore. this paper will continue and extend the investigations of Kasahara, Isaacson, and Stoker (abbreviated as K.I.S.).

We shall deal with the problem under various initial and boundary conditions using a more accurate treatment of the front than K.I.S. together with a rezoning technique for the frontal marker particles. We are thus able to continue the solution for considerably longer times than K.I.S. did. In fact all calculations were carried out until the front crossed over on itself, i.e. until occlusion occurred. Furthermore the Lax-Wendroff type methods used do not require the additional smoothing that Grammeltvedt needed and so local properties are more accurately represented. It is planned to incorporate this theory into a large scale model for the circulation of the atmosphere. The motion of fronts could then be followed by using a refined mesh in the neighborhood of the front. Ciment (1971) has shown that difference schemes with uneven mesh spacings are stable, in the linear case, for dissipative schemes as the Lax-Wendroff method used in these dalculations. Hence, it is numerically feasible to use mesh refinements in the neighborhood of the front.

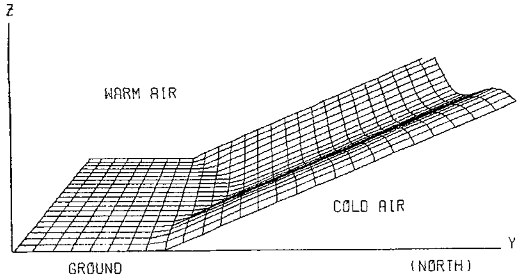

Fig. 1. Vertical height of the two layers.

2. Differential equations

Eliminating the influence of the warm air on the cold air Stoker (1957) derived the following set of equations.

$$u_t + uu_x + vu_y + g\left(1 - \frac{\varrho'}{\varrho}\right) h_x = fv$$

$$v_t + uv_x + vv_y + g\left(1 - \frac{\varrho'}{\varrho}\right) h_y = -f\left(u - \frac{\varrho'}{\varrho}\bar{u}'\right) \quad (1)$$

$$h_t + (hu)_x + (hv)_y = 0$$

u and v are the velocities of the cold air in the x and y directions respectively, h is the height of the cold air layer, ϱ and ϱ' are the densities of the cold and warm air masses, respectively; f is the Coriolis parameter and $\bar{u}'$ is the speed in the x direction of the warm air.

It is assumed that the cold air lies above a region D of the x, y plane and that this region is bounded on the fourth side by a curve $C(t)$. The curve $C(t)$: $(x_C(t), y_C(t))$ defines the front, it is the line along which $h=0$. The points of C move in time with the velocity (u_C, v_C) of the particles on the front: Hence the following conditions hold along C:

$$h = 0$$

$$\frac{d}{dt}(x_C(t)) = u_C(x_C, y_C, t) \quad (2)$$

$$\frac{d}{dt}(y_C(t)) = v_C(x_C, y_C, t)$$

where d/dt is the particle derivative. Along the northern boundary the north-south component of the velocity, v, is specified; it is not necessarily zero as was assumed in K.I.S. At the eastern and western boundaries periodicity is used.

A complete formulation of the problem requires appropriate initial data for u, v, h and the position of the curve $C(t)$. In case 1 u and v are initially the same as for the constant steady state zonal solution while h varies linearly in y and sinusoidally in x.

The initial conditions are thus:

Case 1 (constant state)

$$y_C = C_2 - C_1 \cos\left(\frac{2\pi}{X}x\right)$$

$$u = \bar{u}$$

$$v = 0$$

$$h = (y - y_C)H,\ y_C \leqslant y \leqslant Y$$

where

$$H = \frac{f}{g\left(1 - \frac{\varrho'}{\varrho}\right)}\left(\frac{\varrho'}{\varrho}\bar{u}' - \bar{u}\right);\ \frac{\varrho'}{\varrho}\bar{u}' > \bar{u}.$$

X, Y denote the lengths of the sides of D in the x and y directions respectively. The contour lines of the initial value of h, at 5 000 foot intervals, are plotted in Fig. 2*a*.

As a second case, a physically more realistic condition is assumed, namely that the wind field is initially geostrophic. Thus, at $t=0$ there is no acceleration in either the x or y direction, i.e. $du/dt = dv/dt = 0$. This leads to the following initial conditions.

Case 2 (Geostrophic)

$$h = \frac{y - y_C}{Y - y_C}(Y - b)H$$

$$u = -\frac{g\left(1 - \frac{\varrho'}{\varrho}\right)}{f}\frac{\partial h}{\partial y} + \frac{\varrho'}{\varrho}\bar{u}'$$

$$v = \frac{g\left(1 - \frac{\varrho'}{\varrho}\right)}{f}\frac{\partial h}{\partial x}$$

where $b = C_1 + C_2$ and H, Y, y_C are as in Case 1. The contour lines of the initial value of h for Case 2 is plotted in Fig. 4*a*.

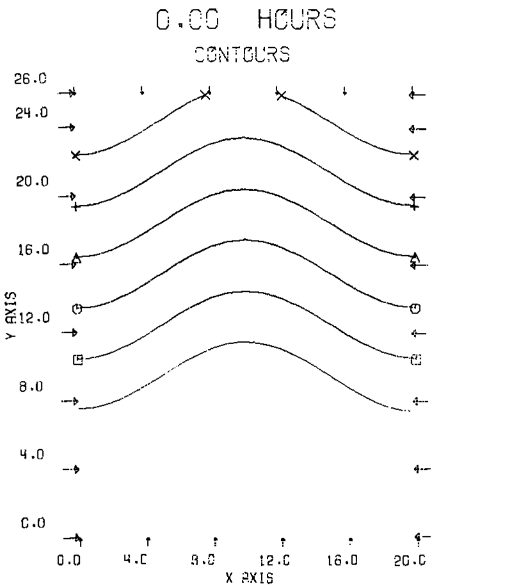

Fig. 2a. Initial height contour pattern, in 5 000 foot intervals, for case 1*a* with no air entering from the north.

Subcases 1*a* and 2*a* denote the problems with periodic east-west boundary conditions and $v=0$ at the northern boundary. Subcases 1*b* and 2*b* denote the same problems but with v specified (non zero) at the north. Finally, subcase 2*c* concerns a problem where the sinusoidal variations initially occur only in the middle third (in the x direction) of the domain.

3. Difference equations

A dimensionless moving coordinate system is introduced so that in dimensionless units the unrefined mesh has length and width equal to 1 (see K.I.S. or Turkel, 1970). By D_Δ is meant the connected set of net points in the interior of D, the region under the cold air. By a regular point is meant a point in D_Δ whose eight surrounding neighbors are all in D_Δ. All other points in D are called irregular points. At regular points, a two step scheme due to Burstein (1964) was used, while at the northern boundary and irregular points sufficiently far from the front, variations of the Lax–Wendroff method were used. At irregular points less than one quarter mesh width from the front the values of u, v and h were found by interpolation. A more detailed analysis of the numerical techniques can be found in Burstein & Turkel (1975).

4. Boundary treatment

The finite difference approximations at the boundaries are considered next. The east and west boundaries consist of regular net points upon using the periodicity condition. Along the northern boundary v is given, while u and h are calculated by using one-sided differences.

The front is defined by a series of discrete Lagrange particles which are allowed to move freely throughout the fixed Eulerian mesh. Between these particles the position of the front is determined by interpolation. The major difficulty presented by this study is following the movement of the front especially as occlusion occurs and severe distortions in the cold air accompanies it. The author has tried many different methods for calculating the dependent variables both in the interior and along the free surface. All these methods give similar results, for case 1, up to 8 hours and for up to 11 hours for case 2. Thus, if one wishes to extend the calculations beyond those given by both K.I.S. and Ritter extra care must be taken to accurately calculate the frontal motion.

Severe distortions create the necessity for rezoning techniques similar to those used by Lagrangian schemes. The advantage of a Eulerian method is that the rezone is one dimensional and there is no need for mass mapping. In order to accomplish the rezoning we introduce a measure of arclength along the front defined by

$$s_{i+1}-s_i=\int_x^{x_{i+1}}\left(1+\left(\frac{dy}{dx}\right)^2\right)^{1/2}dx \qquad (3)$$

where (x_i, y_i) are the coordinates of the ith Lagrange frontal particle. Since we are using a second order scheme we assume that y is a quadratic function of x. When the slope of the front is greater than 1 the roles of x and y are reversed. Thus,

$$y(x)=ax^2+bx+c=\frac{y_{i-1}(x-x_i)(x-x_{i+1})}{(x_{i-1}-x_i)(x_{i-1}-x_{i+1})}$$

$$+ y_i \frac{(x - x_{i-1})(x - x_{i+1})}{(x_i - x_{i=1})(x_i - x_{i+1})}$$

$$y_{i+1} \frac{(x - x_{i-1})(x - x_i)}{(x_{i+1} - x_{i-1})(x_{i+1} - x_i)};$$

$$x_i \leqslant x < x_{i+1} \quad (4)$$

with periodicity near the end points. Since this formula is used only when $(dy/dx)_i$ is less than or equal to one the denominators that occur are usually well behaved. In unusual cases, where there are many oscillations in the front, a linear relationship between x and y is assumed. Since this occurs only at isolated points in time and space the second order accuracy of the method is not affected. When this quadratic form for $y(x)$ is inserted in the arclength integral the integration can be carried out explicitly and

$$s_{i+1} - s_i = \frac{1}{4a} \{(2ax + b)(4a^2x^2 + 4abx + b^2 + 1)^{1/2} + \operatorname{arcsinh}(2ax + b)\}_{x_i}^{x_{i+1}}$$

The arclength of the total front is then determined by letting $s_1 = 0$.

With the arclength thus defined we are in a position to redistribute the frontal particles whenever the distortion becomes too large. When the arclength between any two Lagrange points differs by more than 25% from the average arclength then a redistribution of the points is carried out. It is also possible to rezone portions of the front rather than the entire front. This becomes necessary when sharp corners appear and it is not desirable to introduce any communication between different parts of the free surface. When the rezone is done new Lagrange particles are defined at positions equally spaced in terms of arclength. The coordinates of these new points as well as their velocities are evaluated by quadratic interpolation in terms of arclength from the values at the old Lagrange particles.

The arclength is also used in the evaluation of the slope of the front. Thus,

$$\left(\frac{dy}{dx}\right)_i = \left(\frac{dy}{ds}\right)_i \Big/ \left(\frac{dx}{ds}\right)_i$$

where the derivatives on the right hand side are evaluated by assuming that both x and y are cubic polynomials in s. Cubic polynomials are used rather than quadratic ones to insure symmetry. When x is rather independent of s a linear relationship is used. This creates no difficulties since in this case the front is closely approximated by a straight line in the vicinity of this Lagrange particle.

The introduction of the arclength gives much greater accuracy as the occlusion process continues and sharp changes in the slope of the front appear. Thus, we are able to continue our numerical integrations for periods of time more than twice that achieved by K.I.S. In fact all calculations were carried out until occlusion actually occurred. For times beyond this, changes in the physical model are necessary to account for the multivalved functions that occur.

Along the front the sound speed is zero and so the characteristic directions coincide with the particle path. Thus, u and v cannot be found by extrapolation along the characteristics but must be found by solving the differential equations (2) for u and v along the front.

An implicit method based on the trapezoidal rule, is used to solve the ordinary differential equations. The accuracy of this method is consistent with the second order accuracy of the Lax–Wendroff method. The trapezoidal method does not require information at previous time levels and so presents no difficulties when the points along the front are redistributed.

5. Results

All the figures shown are in a coordinate system that moves to the east with the speed of 10 feet per second except where explicitly noted otherwise. Each mesh is 250 000 feet square (approximately 50 miles). In all cases occlusion occurred and the graphs shown are at times shortly before this.

Fig. 2*b* shows subcase 1*a* after 18 hours. The entire front progresses to the east with the cold front moving eastward faster than the warm front. The front is no longer a single-valued function of the x-coordinate but is curling counterclockwise. The development of this asymmetry characterizes the occlusion process of frontal cyclones.

This subcase assumed that no air enters from the north. The problem was then solved for subcase $1b$ where cold air enters the region from the north simulating a polar wind. As in Alterman & Isaacson, the velocity v is given by

$$v(t, x, Y) = \begin{cases} V_p\left[\cos\left(\frac{\pi t}{T}\right) - 1\right], & t < 2T \\ 0, & t \geqslant 2T \end{cases} \tag{5}$$

Fig. 3 shows the result after 18 hours with $T = 7$ hours and $V_p = 10$ ft./sec. As expected the polar air forces the front southward. The front becomes steeper and the cyclonic activity increases. Replacement of formula (5) by a periodic function in time had no appreciable affect on the occlusion process, though the length of the period did affect the time required for occlusion to occur. It seems reasonable that if the velocity at the northern boundary were sufficiently negative then occlusion would not occur. In all cases the propogation of disturbances is faster towards the north since the sound speed is proportional to the square root of the height of the cold air. This height increases approximately linearly towards the north (see for example Fig. 8).

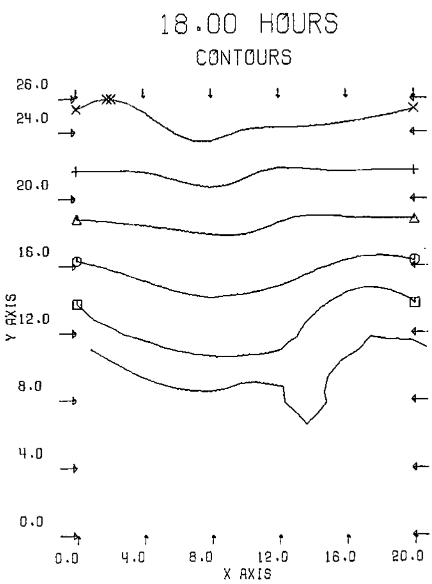

Fig. 2b. Height contour pattern for case $1a$ after 18 hours.

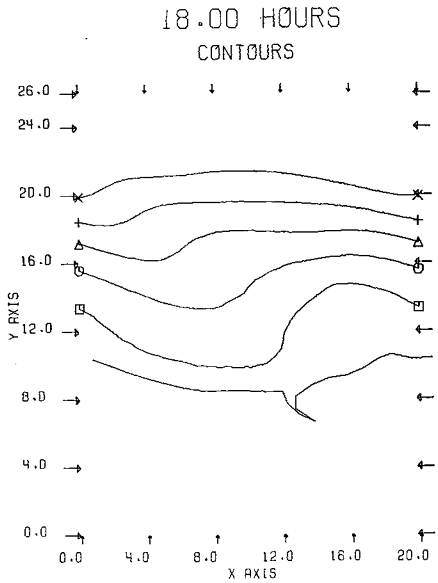

Fig. 3. Height contour pattern for case $1b$, air entering from the north, after 18 hours.

In case 2 the initial velocities and height field distribution are geostrophic. The initial shape of the front is again sinusoidal with the height contour lines flattening out towards the north as seen in Fig. $4a$. Fig. $4b$ displays the height contour lines after 24 hours. As before the entire frontal system progresses eastward. It takes longer for the occlusion process to occur since the initial accelerations are zero. However, after a complete day the occlusion process is well developed and there are large cyclonic motions. In subcase $2b$ we consider the effect of a polar wind entering from the north as given by eq. (5). Fig. 6 shows the contour levels for the height field after 24 hours.

The periodic east-west boundary conditions are not realistic for a single wave of period X. Therefore, in subcase $2c$ a larger region is introduced to simulate an infinite domain in the x direction. That is, X is chosen as 60 dimensionless units; while the initial data is chosen to be: a single wave of period $X/3$ over the center twenty units and extended to the right and left with values independent of x (see Fig. $6a$). In Fig. $6b$ it is seen that the occlusion process is not greatly affected, after 24 hours, by this change in initial and boundary conditions. In the regions away from the occlusion

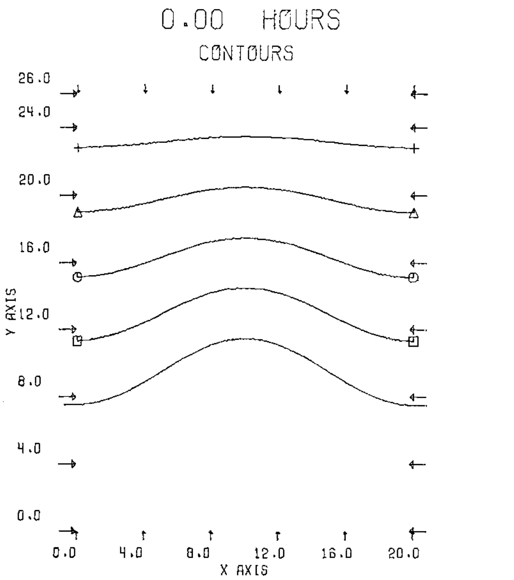

Fig. 4a. Initial height contour pattern, in 5 000 foot intervals, for case $2a$ with geostrophic initial conditions.

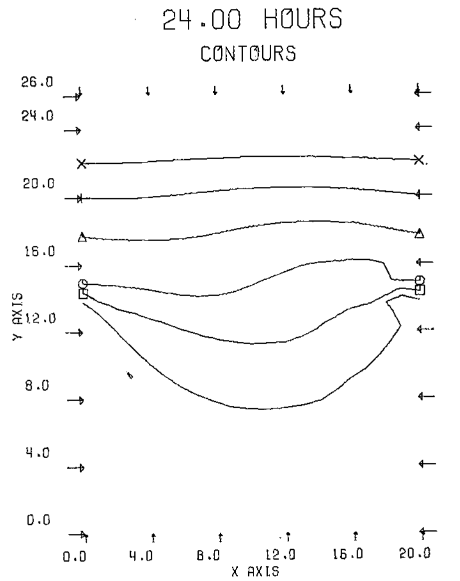

Fig. 5. Height contour pattern for case $2b$ after 24 hours.

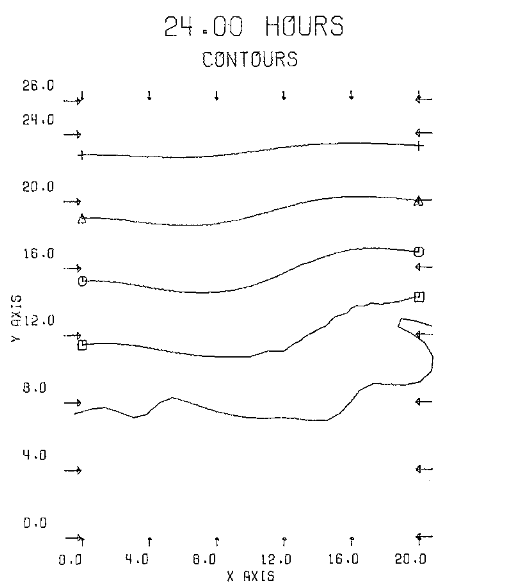

Fig. 4b. Height contour pattern for case $2a$ after 24 hours.

process the front remains closer to its initial state and even moves slightly southward. Fig. 6c shows the center portion of Fig. 6b to facilitate comparisons with the other graphs. In Fig. 7 is shown the velocity field after 24 hours for the geostrophic initial conditions (case $2a$). In this plot the circulation pattern is readily visible. The magnitude of the arrows is proportional to the speed, while the direction of the arrow is parallel to the velocity vector. Finally, in Fig. 8 is plotted the height field in a three

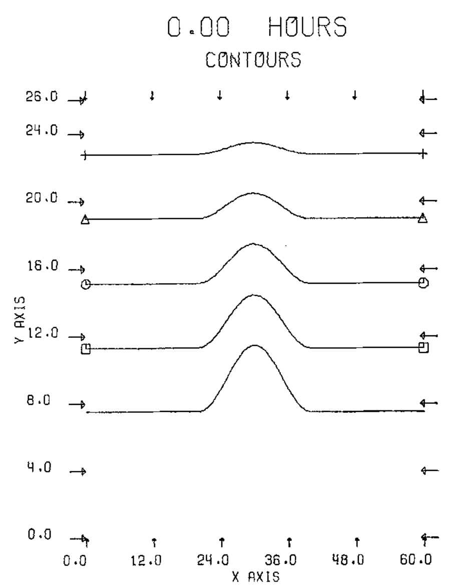

Fig. 6a. Initial height contour pattern for case $2c$.

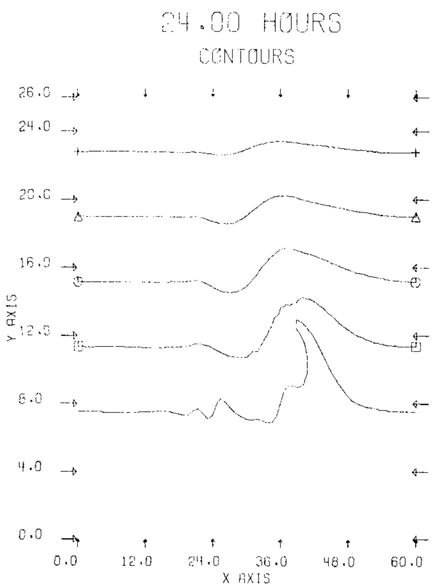

Fig. 6b. Height contour pattern for case 2*c* after 24 hours.

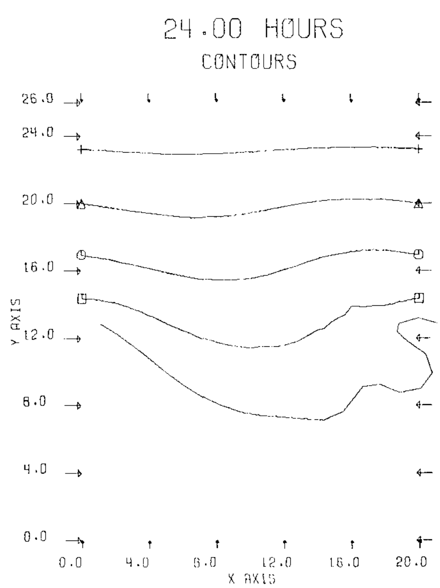

Fig. 6c. Central portion of Fig. 6*b*.

dimensional perspective graph for subcase 2*b* after 24 hours (this corresponds to Fig. 5). The distortions caused by the occlusion process are readily visible.

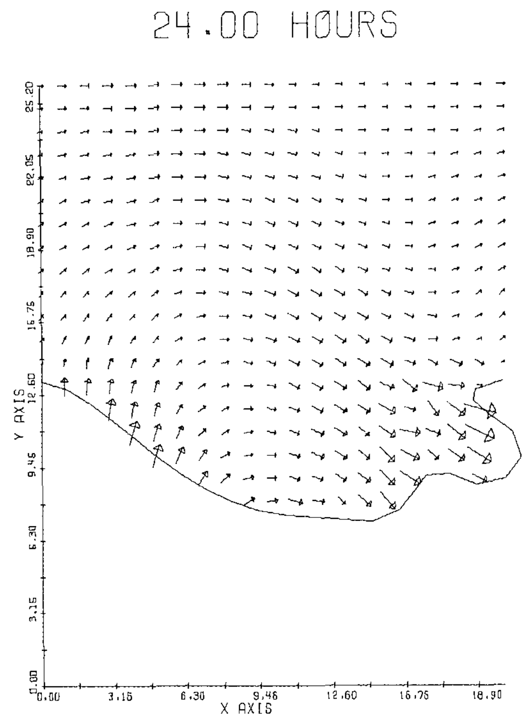

Fig. 7. Velocity field for case 2*a* after 24 hours.

6. Conclusions

The motion of cold fronts in the atmosphere can be described by a system of nonlinear equations for the motion of a single layer of fluid. These equations include gravitational and Coriolis forces but ignore thermodynamic variables. By changing the initial and boundary conditions the shape of the front, the cyclonic pattern of the air and the time variation can all be altered. Within one day the cyclonic pattern is clearly developed for realistic initial conditions. Thus, this model indicates that the action of purely mechanical forces are primarily

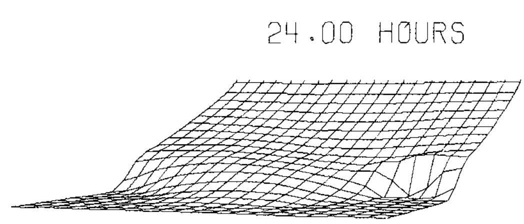

Fig. 8. Three-dimensional perspective plot of the height field for case 2*b* after 24 hours.

responsible for the features of the occlusion process. Furthermore, since this model is relatively simple the scheme can be incorporated as a subset of a global model with little extra computational effort. With the extra resolution provided frontal motion can be accurately followed for periods of greater than 24 hours without any smearing of details.

Acknowledgement

The author wishes to thank Professors E. Isaacson and J. J. Stoker without whose advice and encouragement this work could not have been completed.

REFERENCES

Abdullah, A. J. 1949. Cyclogenesis by a Purely Mechanical Process. *J. Meteor. 6*, 86–97.

Alterman, Z. S. & Isaacson, E. 1969. A method for calculating frontal motion, one dimensional tests. *J. Comp. Phys. 4*, 67–96.

Burstein, S. Z. 1967. High order accurate difference methods in hydrodynamics. In *Nonlinear partial differential equations* (ed. W. F. Ames), pp. 279–290. Academic Press, New York.

Burstein, S. Z., Turkel, E., 1975. Numerical Methods for Mixed Initial Boundary Value Problems in Deformable Media. To be Published.

Ciment, M. 1971. Stable difference schemes with uneven mesh spacings. *Math. Comp. 25*, 219–227.

Freeman, J. C. 1952. Flow under an inversion in middle lattitudes. Ph.D. Dissertation, Dept. Meteorology, University of Chicago. 52 pp.

Grammeltvedt, A. 1970. Numerical simulation of the motion of atmospheric fronts using a two layer model. *Tellus 22*, 627–37.

Kasahara, A., Isaacson, E. & Stoker, J. J. 1965. Numerical studies of frontal motion in the atmosphere. *Tellus 17*, 261–76.

Kasahara, A. & Rao, D. B. 1972. Instability of frontal motions in the atmosphere. *J. Atmos. Sci. 29*, 1090–1108.

Lax, P. D. & Wendroff, B. 1964. Difference schemes for hyperbolic equations with higher order accuracy. *Comm. Pure Applied Math. 17*, 381–98.

Ritter, Z. W. 1970. A Langrangian method for calculating problems in meteorology. *J. Comp. Phys. 6*, 510–526.

Stoker, J. J. 1957. *Water waves.* Interscience-Wiley, New York. 567 pp.

Tepper, M. 1952. The application of the hydraulic analogy to certain atmospheric flow problems. US Dept. Commerce, Weather Bureau Research, Paper No. 35, 50 pp.

Turkel, E. 1970. Frontal motion in the atmosphere. Courant Inst. Math. Sci., New York Univ. Report No. IMM-385.

ФРОНТАЛЬНЫЕ ДВИЖЕНИЯ В АТМОСФЕРЕ

На основе однослойной нелинейной модели, предложенной Стокером, изучается движение фронтальных возмущений в атмосфере. Уравнения движения интегрируются внутри области двухшаговым методом. Течения, возникающие при различных начальных и граничных условиях, рассматриваются за значительно более долгие времена, чем рассчитывалось ранее. Граница раздела прослеживается путем численной процедуры, позволяющей рассматривать произвольную форму фронта. Поэтому течения могут описываться вплоть до момента возникновения окклюзии, что позволяет выяснить влияние различных начальных и граничных условий на процесс окклюзии. Во всех случаях холодный фронт распространяется быстрее теплого и позади холодного фронта существует область относительно сильной конвергенции масс. Вблизи холодного фронта ясно видна циркуляция циклонического типа. Из этих фактов следует, что сильные штормы связаны с холодными, а не с теплыми фронтами.